

Astrophysical  $S_{E2}$  factor of the  $^{12}\text{C}(\alpha, \gamma)^{16}\text{O}$  reaction through the  $^{12}\text{C}(^{11}\text{B}, ^7\text{Li})^{16}\text{O}$  transfer reaction

Y. P. Shen (谌阳平),<sup>1</sup> B. Guo (郭冰),<sup>1,\*</sup> Z. H. Li (李志宏),<sup>1</sup> Y. J. Li (李云居),<sup>1</sup> D. Y. Pang (庞丹阳),<sup>2,3</sup> S. Adhikari,<sup>4</sup> Z. D. An (安振东),<sup>5</sup> J. Su (苏俊),<sup>1</sup> S. Q. Yan (颜胜权),<sup>1</sup> X. C. Du (杜先超),<sup>1</sup> Q. W. Fan (樊启文),<sup>1</sup> L. Gan (甘林),<sup>1</sup> Z. Y. Han (韩治宇),<sup>1</sup> D. H. Li (李东辉),<sup>1</sup> E. T. Li (李二涛),<sup>6</sup> X. Y. Li (李鑫悦),<sup>1</sup> G. Lian (连钢),<sup>1</sup> J. C. Liu (刘建成),<sup>1</sup> T. L. Ma (马田丽),<sup>1</sup> C. J. Pei (裴常进),<sup>1</sup> Y. Su (苏毅),<sup>1</sup> Y. B. Wang (王友宝),<sup>1</sup> S. Zeng (曾晟),<sup>1</sup> Y. Zhou (周勇),<sup>1</sup> and W. P. Liu (柳卫平)<sup>1</sup>

<sup>1</sup>China Institute of Atomic Energy, P. O. Box 275(10), Beijing 102413, China


<sup>2</sup>School of Physics and Nuclear Energy Engineering, Beihang University, Beijing 100191, China

<sup>3</sup>Beijing Key Laboratory of Advanced Nuclear Materials and Physics, Beihang University, Beijing 100191, China

<sup>4</sup>Physics Department, Techno India University, Kolkata 700091, India

<sup>5</sup>School of Physics and Astronomy, Sun Yat-Sen University, Zhuhai 519082, China

<sup>6</sup>College of Physics and Energy, Shenzhen University, Shenzhen 518060, China

 (Received 26 April 2017; revised manuscript received 13 November 2018; published 19 February 2019)

The  $^{12}\text{C}(\alpha, \gamma)^{16}\text{O}$  reaction plays a key role in the evolution of stars with masses of  $M > 0.55 M_{\odot}$ . The cross-section of the  $^{12}\text{C}(\alpha, \gamma)^{16}\text{O}$  reaction within the Gamow window ( $E_{\text{c.m.}} = 300$  keV,  $T_9 = 0.2$ ) is extremely small (about  $10^{-17}$  barn), which makes the direct measurement in a ground-based laboratory with existing techniques unfeasible. Up until now, the cross-sections at lower energies can only be extrapolated from the data at higher energies. However, two subthreshold resonances, located at  $E_x = 7.117$  MeV and  $E_x = 6.917$  MeV, make this extrapolation more complicated. In this work, the 6.917 MeV subthreshold resonance in the  $^{12}\text{C}(\alpha, \gamma)^{16}\text{O}$  reaction was investigated via the  $^{12}\text{C}(^{11}\text{B}, ^7\text{Li})^{16}\text{O}$  reaction. The experiment was performed using the Q3D magnetic spectrograph at the HI-13 tandem accelerator. We measured the angular distribution of the  $^{12}\text{C}(^{11}\text{B}, ^7\text{Li})^{16}\text{O}$  transfer reaction leading to the 6.917 MeV state. Based on the finite-range distorted wave Born approximation (FRDWBA) and coupled-reaction-channel (CRC) analysis, we derived the asymptotic normalization coefficient (ANC) of the 6.917 MeV level in  $^{16}\text{O}$  to be  $(1.10 \pm 0.29) \times 10^{10} \text{ fm}^{-1}$ , with which the reduced  $\alpha$  width was computed to be  $18.0 \pm 4.7$  keV at the channel radius of 6.5 fm. Finally, we calculated the astrophysical  $S_{E2}(300)$  factor of the ground-state transitions to be  $46.2 \pm 7.7$  keV b. The result for the astrophysical  $S_{E2}(300)$  factor confirms the values obtained in various direct and indirect measurements and presents an independent examination of the most important data in nuclear astrophysics.

DOI: [10.1103/PhysRevC.99.025805](https://doi.org/10.1103/PhysRevC.99.025805)

## I. INTRODUCTION

The  $^{12}\text{C}(\alpha, \gamma)^{16}\text{O}$  reaction is believed to be one of the most crucial reactions in nuclear astrophysics [1–3]. Following the production of  $^{12}\text{C}$  by the triple- $\alpha$  process, it strongly influences the ratio of the abundances for the main isotopes of carbon and oxygen ( $^{12}\text{C}$  and  $^{16}\text{O}$ ) which are the fourth- and third-most abundant nuclei in the visible universe. The C/O ratio at the end of helium burning affects not only the production of all elements heavier than  $A = 16$ , but also the explosion of supernovae [1]. While the cross-section for the triple- $\alpha$  process is experimentally well determined [4,5], the cross-section of the  $^{12}\text{C}(\alpha, \gamma)^{16}\text{O}$  reaction taking place in the helium burning phase ( $T_9 = 0.2$ ) is now thought to be with the most serious uncertainty in nucleosynthesis [6]. The Gamow peak for the  $^{12}\text{C}(\alpha, \gamma)^{16}\text{O}$  reaction at  $T_9 = 0.2$  is located at  $E_{\text{c.m.}} = 300$  keV. Stellar modeling requires the uncertainty for the  $^{12}\text{C}(\alpha, \gamma)^{16}\text{O}$  cross-section at  $E_{\text{c.m.}} = 300$  keV to be better than 10% [1,7], while the present uncertainty is approximately 20% [8].

At energies within the Gamow window, the  $^{12}\text{C}(\alpha, \gamma)^{16}\text{O}$  cross-sections are too low (on the order of  $10^{-17}$  barn) to be measured directly in a ground-based laboratory. Although, in the near future, a direct measurement is planned by the JUNA collaboration [9], all direct measurements so far have been done at energies higher than  $E_{\text{c.m.}} = 890$  keV [10–12]. How to achieve a reliable extrapolation of the cross-sections from higher energies to the Gamow window has been a long-standing problem. Furthermore, two subthreshold resonances, 7.117 MeV  $1^-$  and 6.917 MeV  $2^+$ , make this extrapolation more complicated. There are two main capture modes in the  $^{12}\text{C}(\alpha, \gamma)^{16}\text{O}$  reaction. One is the  $E1$  transition to the ground state that includes the contributions from the low-energy tail of the broad  $1^-$  resonance at  $E_x = 9.585$  MeV and the subthreshold  $1^-$  resonance at  $E_x = 7.117$  MeV. The other is the  $E2$  transition to the ground state, which mainly stems from the direct capture and the subthreshold  $2^+$  resonance at  $E_x = 6.917$  MeV. The states with identical multipolarity interfere with each other.  $R$ -matrix analysis is a widely used method to deal with the situations that require level parameters (i.e., energies, ANCs, and lifetimes). Indirect techniques are believed to be quite valuable since they can be used to deduce these

\* guobing@ciae.ac.cn

level parameters [13]. To date, considerable indirect methods have been utilized to study these two subthreshold resonances, such as the  $\alpha + {}^{12}\text{C}$  elastic scattering [14], the  $\beta$ -delayed  $\alpha$  decay of  ${}^{16}\text{N}$  [15], transfer reactions [16], and Coulomb dissociation [17]. All of these results for the  $S_{E2}(300)$  factor vary from 36 to 85 keV b.

Due to the importance of the transfer reaction method to evaluate the  ${}^{12}\text{C}(\alpha, \gamma){}^{16}\text{O}$  reaction, a lot of work has been done [16,18–31] to date. Pühlhofer *et al.* [18] measured the angular distributions of  ${}^{12}\text{C}({}^7\text{Li}, \text{t}){}^{16}\text{O}$  at  $E_{\text{lab}} = 15, 21.1,$  and  $24$  MeV and the reduced  $\alpha$ -widths of some states were extracted. Johnson *et al.* [19] measured the  ${}^{12}\text{C}({}^6\text{Li}, \text{d}){}^{16}\text{O}$  reaction within an energy range from 5.6 to 14.0 MeV. However, the events of  ${}^{12}\text{C}({}^6\text{Li}, \text{d}){}^{16}\text{O}_{6.92}$  could not be distinguished from the events of  ${}^{12}\text{C}({}^6\text{Li}, \text{d}){}^{16}\text{O}_{7.12}$  and no further analysis such as finite-range distorted wave Born approximation (FRDWBA) was made. The  ${}^{12}\text{C}({}^7\text{Li}, \text{t}){}^{16}\text{O}$  reaction was measured in Cobern *et al.*'s [20] work, but they were also unable to separate the events corresponding to 6.92 and 7.12 MeV states. Cunsolo *et al.* [23] measured the  ${}^{12}\text{C}({}^6\text{Li}, \text{d}){}^{16}\text{O}$  reaction in the 20–34 MeV incident energy range and analyzed in terms of Hauser-Feshbach and FRDWBA theories. Becchetti *et al.* [21,22] measured the  ${}^{12}\text{C}({}^6\text{Li}, \text{d}){}^{16}\text{O}$  and  ${}^{12}\text{C}({}^7\text{Li}, \text{t}){}^{16}\text{O}$  reactions at energies of 42 and 34 MeV, respectively. Becchetti *et al.* [24] measured the  ${}^{12}\text{C}({}^6\text{Li}, \text{d}){}^{16}\text{O}$  reaction again at the energy of 90 MeV. The Hauser-Feshbach and FRDWBA theories were applied in the analysis. Brune *et al.* [25] measured the  ${}^{12}\text{C}({}^6\text{Li}, \text{d}){}^{16}\text{O}$  and  ${}^{12}\text{C}({}^7\text{Li}, \text{t}){}^{16}\text{O}$  reactions to the bound  $2^+$  and  $1^-$  states of  ${}^{16}\text{O}$  and analyzed these data using the FRDWBA code FRESKO [32]. Drummer *et al.* [26] measured the  ${}^{12}\text{C}({}^6\text{Li}, \text{d}){}^{16}\text{O}_{g.s.}$  reaction with a polarized  ${}^6\text{Li}$  beam. Keeley *et al.* [27] measured  ${}^{12}\text{C}({}^6\text{Li}, \text{d}){}^{16}\text{O}$  at 34 and 50 MeV and analyzed the multistep contributions to the transfers leading to the  $0^+, 2^+, 4^+,$  and  $3^-$  states. Belhout *et al.* [28] measured  ${}^{12}\text{C}({}^6\text{Li}, \text{d}){}^{16}\text{O}$  at the energy of 48.2 MeV and analyzed it using the FRDWBA theory with a particular emphasis put on the states of astrophysical interest, mainly, the 7.12 MeV state. Oulebsir *et al.* [30] measured the  ${}^{12}\text{C}({}^7\text{Li}, \text{t}){}^{16}\text{O}$  reaction at two incident energies of 28 and 34 MeV and analyzed this using the Hauser-Feshbach and FRDWBA theories. Adhikari *et al.* [16,29] measured  ${}^{12}\text{C}({}^6\text{Li}, \text{d}){}^{16}\text{O}$  at 9 and 20 MeV, and continuum discretized coupled channel-coupled reaction channel (CDCC-CRC) calculations have been used to analyze the data. Avila *et al.* [31] applied the  $\alpha$ -transfer reaction  ${}^6\text{Li}({}^{12}\text{C}, \text{d}){}^{16}\text{O}$  with inverse kinematics and constrained the 6.05 and 6.13 MeV cascade transitions in the  ${}^{12}\text{C}(\alpha, \gamma){}^{16}\text{O}$  reaction. Particularly, the  $S_{E2}(300)$  factors were extracted in Refs. [16,25,28,30]. As mentioned above, all of the works were performed with the  ${}^{12}\text{C}({}^6\text{Li}, \text{d}){}^{16}\text{O}$  and  ${}^{12}\text{C}({}^7\text{Li}, \text{t}){}^{16}\text{O}$  transfer systems. It is known that one of the largest sources of uncertainty in the ANC determination from these studies is the uncertainty in the FRDWBA model. For this reason, measurements of different types of transfer reactions may help us to better understand the systematic uncertainties in the model and lead to improvement in the method. Additional measurement via independent transfer reactions is therefore desirable. In addition to the  $({}^6\text{Li}, \text{d})$  and  $({}^7\text{Li}, \text{t})$  reactions, the  $({}^{11}\text{B}, {}^7\text{Li})$  transfer reaction is another choice for research in  $(\alpha, \gamma)$  or  $(\alpha, n)$  reactions, which has been successfully applied

to the research of  ${}^{13}\text{C}(\alpha, n){}^{16}\text{O}$  [33]. In our present work, measurement of the  ${}^{12}\text{C}({}^{11}\text{B}, {}^7\text{Li}){}^{16}\text{O}$  reaction was performed to derive the reduced  $\alpha$ -width of the 6.917 MeV  $2^+$  subthreshold resonance. The astrophysical  $S_{E2}$  factor at the Gamow peak of the  ${}^{12}\text{C}(\alpha, \gamma){}^{16}\text{O}$  reaction was then studied.

## II. EXPERIMENT

The experiment was performed at the HI-13 national tandem accelerator laboratory of the China Institute of Atomic Energy (CIAE) in Beijing. The experimental setup and procedures were similar to those previously reported [33–36]. The  ${}^{11}\text{B}$  beam with an energy of 50 MeV was delivered and utilized to measure the angular distribution of the  ${}^{12}\text{C}({}^{11}\text{B}, {}^7\text{Li}){}^{16}\text{O}$  reaction leading to the excited state of  ${}^{16}\text{O}$  at  $E_x = 6.917$  MeV and  ${}^{11}\text{B} + {}^{12}\text{C}$  elastic scattering. A self-supporting  ${}^{12}\text{C}$  target with a thickness of  $66 \pm 5 \mu\text{g}/\text{cm}^2$  was used in the present experiment. In addition, the  ${}^7\text{Li}$  beam with an energy of 26 MeV and a  $\text{SiO}_2$  target with a thickness of  $86 \pm 7 \mu\text{g}/\text{cm}^2$  were used for the measurement of the angular distribution of the  ${}^7\text{Li} + {}^{16}\text{O}$  elastic scattering. The reaction products were focused and separated by the Q3D magnetic spectrograph. A two-dimensional position sensitive silicon detector (X1) was fixed at the focal plane of Q3D. The two-dimensional position information from X1 enabled the products emitted into the acceptable solid angle to be completely recorded, and the energy information was used to remove the impurities with the same magnetic rigidity. As an example, Fig. 1 displays the focal-plane position spectrum of  ${}^7\text{Li}$  at  $\theta_{\text{lab}} = 10^\circ$  from the  ${}^{12}\text{C}({}^{11}\text{B}, {}^7\text{Li}){}^{16}\text{O}$  reaction. We

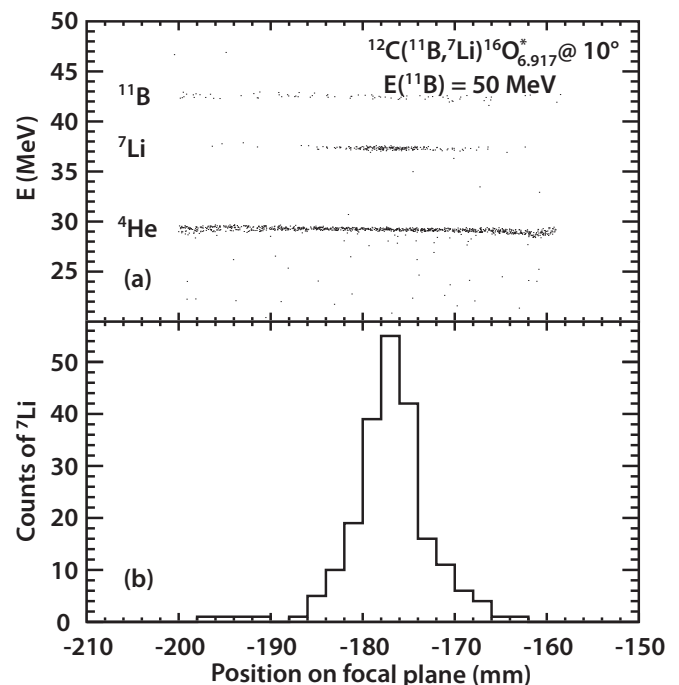


FIG. 1. Focal-plane position spectrum of  ${}^7\text{Li}$  at  $\theta_{\text{lab}} = 10^\circ$  from the  ${}^{12}\text{C}({}^{11}\text{B}, {}^7\text{Li}){}^{16}\text{O}$  reaction. (a) Two-dimensional spectrum of energy vs. focal-plane position. (b) Spectrum gated by the  ${}^7\text{Li}$  events in (a).

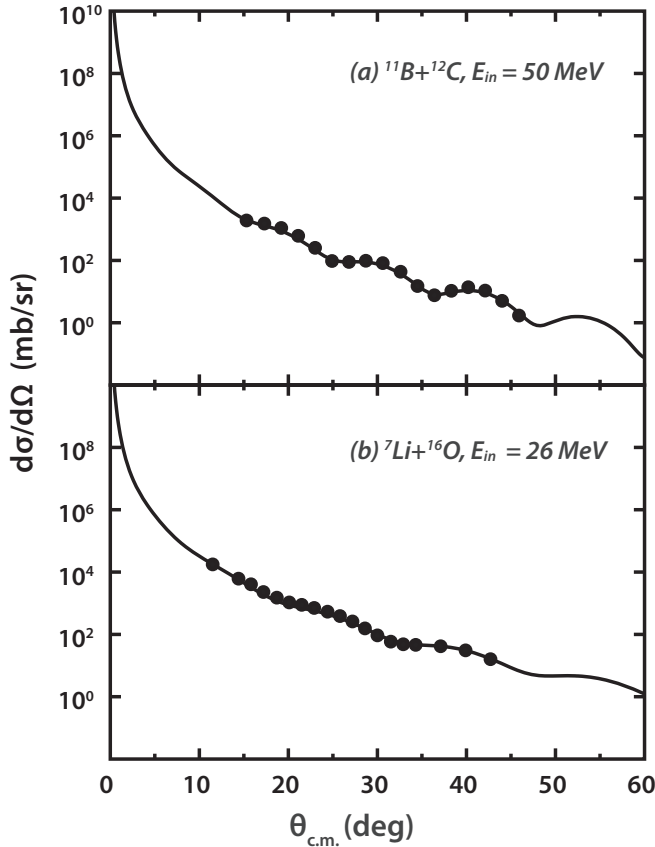


FIG. 2. The experimental data and fitting with single-folding potentials of the elastic scattering of  $^{11}\text{B} + ^{12}\text{C}$  [shown in subplot (a)] and  $^7\text{Li} + ^{16}\text{O}$  [shown in subplot (b)], which are the entrance and exit channels of  $^{12}\text{C}(^{11}\text{B}, ^7\text{Li})^{16}\text{O}$ .

found that the energy resolution is approximately 40 keV and the  $^7\text{Li}$  events related to the 6.917 MeV state are well separated from others. The events related to the 7.12 MeV state are about 40 mm away from the events related to the 6.917 MeV state. Since we used one piece of silicon detector with a length of 50 mm, it is difficult to measure the two states in one run. Thus, the data for the 7.117 MeV state are not presented in this work.

We found that the  $^{12}\text{C}$  will build up on the front surface of the target because of the oil vapor in the beam pipe [37]. Apparently, the buildup of  $^{12}\text{C}$  will increase the amount of the  $^{12}\text{C}$  atoms in the target, and influence the determination of the reaction cross-sections. To monitor the possible buildup of  $^{12}\text{C}$ , the  $^{11}\text{B}$  elastic scattering on the  $^{12}\text{C}$  target was measured at the start and the end of the measurement for each angle. Although the amount of  $^{12}\text{C}$  in the target increased by about 9% during the whole measurement, it was less than 2% for the measurement of the cross-sections at a single angle. All the measured cross-sections were corrected for the change in target thickness and the uncertainty of target thickness from the buildup of  $^{12}\text{C}$  was also included in the present work to avoid unexpected systematic error.

To derive the optical potential of the entrance and exit channels of the  $^{12}\text{C}(^{11}\text{B}, ^7\text{Li})^{16}\text{O}$  reaction, we performed

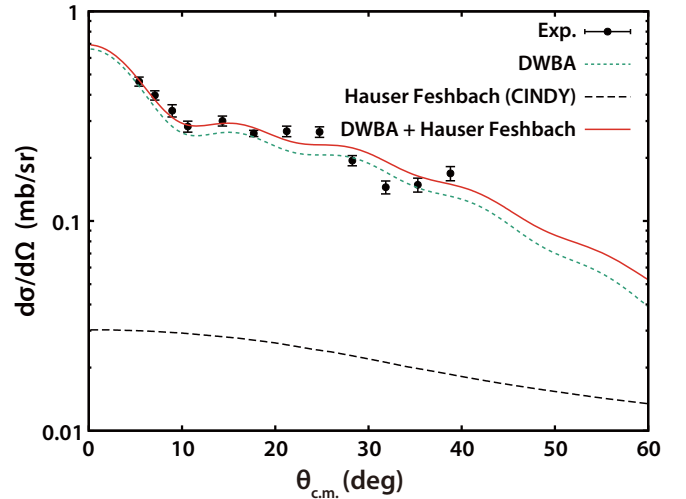


FIG. 3. Angular distribution of the  $^{12}\text{C}(^{11}\text{B}, ^7\text{Li})^{16}\text{O}$  reaction leading to the 6.917 MeV  $2^+$  state of  $^{16}\text{O}$ . The green dashed line and the black dotted line represent the FRDWBA and Hauser-Feshbach calculation, respectively. The red solid line denotes the FRDWBA calculation summed to the compound nuclear component.

measurements of the elastic scattering of the  $^{11}\text{B} + ^{12}\text{C}$  and  $^7\text{Li} + ^{16}\text{O}$  at energies of 50 and 26 MeV, respectively. The data for the differential cross-sections and fitting curves are shown in Fig. 2. In Fig. 3, we also display the angular distribution of the  $^{12}\text{C}(^{11}\text{B}, ^7\text{Li})^{16}\text{O}$  reaction leading to the 6.917 MeV  $2^+$  state of  $^{16}\text{O}$ .

### III. EXTRACTION OF ANC

The FRDWBA calculations were performed to derive the ANC of the 6.917 MeV  $2^+$  subthreshold state in  $^{16}\text{O}$  by using the FRESKO code [32]. The FRDWBA calculations required the optical potentials for the entrance channel ( $^{11}\text{B} + ^{12}\text{C}$ ), exit channel ( $^7\text{Li} + ^{16}\text{O}$ ), and the core-core ( $^7\text{Li} + ^{12}\text{C}$ ) interactions. The real binding potentials for the ( $\alpha + ^7\text{Li}$ ) and ( $\alpha + ^{12}\text{C}$ ) systems were also required. As the depths of the binding potentials would be automatically adjusted during the calculation by the FRESKO code, only the geometrical parameters for the binding potentials were required.

A single-folding model [38,39] was used for the optical model potentials of the entrance and exit channels. Nucleon density distributions of  $^{11}\text{B}$ ,  $^{12}\text{C}$ , and  $^{16}\text{O}$  were obtained using Hartree-Fock calculations with the SkX interaction [40], while those of  $^7\text{Li}$  were taken from a independent-particle model [41]. These density distributions were folded using the systematic nucleon-nucleus potential of the JLMB model [42]. Depths of these single-folding potentials were adjusted by normalizing parameters to provide an optimum reproduction of the experimental data with the optical model. The comparisons of the experimental data with the optical model calculations with these potentials are depicted in Fig. 2. An approximation that we implemented was that the same optical potential was used for both the exit channel and the core-core interaction. The way to prove the correction of this approximation is to compare the difference between

TABLE I. List of parameters and uncertainty budget for the calculation of the spectroscopic factor ( $S_\alpha$ ) and ANC. The main parameters used in the FRDWBA calculation are shown in the first column. The last column,  $\delta_{C^2}$ , represents the uncertainty of the ANC from each parameter.  $N_r$  and  $N_i$  are the normalization factors of the real and imaginary parts of the single-folding potential. The subscripts “en” and “ex” represent the entrance and exit channel, respectively.  $S_x$  represents the spectroscopic amplitude of  $\alpha$  cluster in  $x$ . It is mentioned that there is only one  $\delta_{C^2}$  from each set of  $r_0$  and  $a$  since  $a$  of the bound state is adjusted to reproduce the rms radius of the  $\alpha$ -cluster wave function. “Angle range” represents the different range of angles used in the fit.

Parameter	Value	$\sigma$	$\delta_{C^2}$
$N_{r_{en}}$	1.071	0.034	1.1%
$N_{i_{en}}$	1.388	0.049	0.5%
$N_{r_{ex}}$	0.744	0.063	2.9%
$N_{i_{ex}}$	1.56	0.10	4.9%
$S_{^{11}\text{B}, 3S_0}$	0.64	0.09	13.9%
$S_{^{11}\text{B}, 2D_2}$	0.74	0.09	5.9%
$r_0$ of $^{16}\text{O}$	0.96 fm	0.12 fm	11.4%
$a$ of $^{16}\text{O}$	0.90 fm		
$r_0$ of $^{11}\text{B}$	0.98 fm	0.12 fm	2.9%
$a$ of $^{11}\text{B}$	0.60 fm		
Statistics			10.0%
Target thickness			7.9%
Angle range			2.0%
Channel radius			5.4%
Difference between FRDWBA and CRC			9.1%
Total uncertainty in ANC and $S_\alpha$			26.1%

the prior and post interactions in the FRDWBA calculation. The difference in the present work was less than 1%, which verified our approximation for the core-core optical potential. The uncertainties of the normalizing parameters of the single-folding potentials for entrance and exit channels were evaluated based on a least-square minimization procedure and the total impact of the normalizing parameters on the  $S_\alpha$  and the ANC was found to be approximately 6%. The details of the normalization parameters and the uncertainties are shown in Table I.

The geometric parameters of binding potentials for the ( $\alpha + ^7\text{Li}$ ) and ( $\alpha + ^{12}\text{C}$ ) systems were another important input for the FRDWBA calculation. The geometric parameters, radius  $r_0$  and diffuseness  $a$  for the ( $\alpha + ^7\text{Li}$ ) system, were adjusted to reproduce the root-mean-square (rms) radius ( $\sqrt{\langle r^2 \rangle} = 3.204$  fm) of the  $\alpha$ -cluster wave function using the formula

$$\langle r_B^2 \rangle = \frac{m_{\text{He}}}{m_B} \langle r_{\text{He}}^2 \rangle + \frac{m_{\text{Li}}}{m_B} \langle r_{\text{Li}}^2 \rangle + \frac{m_{\text{He}} m_{\text{Li}}}{m_B^2} \langle r^2 \rangle \quad (1)$$

given in Guo *et al.* (2012) [33], where the rms radii of  $^4\text{He}$ ,  $^7\text{Li}$ , and  $^{11}\text{B}$  were taken to be 1.47, 2.384, and 2.605 fm, respectively [43]. The resulting parameters were  $r_0 = 0.98$  fm and  $a = 0.60$  fm. We investigated the dependence of the calculated  $S_\alpha$  and ANC on the geometric parameters for the ( $\alpha + ^7\text{Li}$ ) system. With a radius between 0.86–1.10 fm, the diffuseness was adjusted to reproduce the rms radius

of 3.204 fm. The impact of this change on the ANC was found to be approximately 3%. The geometric parameters for the ( $\alpha + ^{12}\text{C}$ ) system were deduced following a similar procedure. While the rms radii of  $^4\text{He}$ ,  $^{12}\text{C}$ , and the first  $2^+$  states of  $^{16}\text{O}$  were recommended to be 1.47 fm [43], 2.481 fm [43], and 3.1 fm [44], respectively, the rms radius of the  $\alpha$ -cluster wave function was found to be 4.87 fm. The geometry parameters were deduced to be  $r_0 = 0.96$  fm and  $a = 0.9$  fm. We varied the radius between 0.84–1.08 fm and adjusted diffuseness to reproduce the rms radius of 4.87 fm. The impact of the change on the ANC was found to be approximately 11%. In the works of Oulebsir *et al.* (2012) [30] and Keeley *et al.* (2003) [27], the geometric parameters of the ( $\alpha + ^{12}\text{C}$ ) system were recommended to be  $r_0 = 1.16$  fm,  $a = 0.73$  fm and  $r_0 = 1.25$  fm,  $a = 0.65$  fm, respectively. The above two sets of parameters only caused a change of less than 5% on the ANC, which provided a crosscheck to our geometric parameters.

To obtain the spectroscopic factor and ANC of the  $\alpha$ -cluster in the  $^{16}\text{O}_{6,917}$ , the spectroscopic amplitudes of the  $\alpha$ -cluster in the ground state of  $^{11}\text{B}$  needed to be fixed. The single-particle wave function describing the relative motion between the  $\alpha$ -cluster and the  $^7\text{Li}$  core in the  $^{11}\text{B}$  ground state has two components denoted by quantum numbers  $NL_j = 3S_0$  and  $2D_2$ , respectively. Another experiment was performed on our facilities and the angular distribution of  $^7\text{Li}(^6\text{Li}, d)^{11}\text{B}_{\text{g.s.}}$  at an energy of 24 MeV was measured and analyzed [45]. The spectroscopic amplitudes of these two components were determined to be  $0.64 \pm 0.09$  and  $0.74 \pm 0.09$ . The uncertainties of the ANC from the  $^{11}\text{B}$   $3S_0$  and  $2D_2$  spectroscopic amplitudes were approximately 14% and 6%. The details will be published in a further paper.

The compound nuclear calculations were performed using the Hauser-Feshbach (HF) code CINDY [46]. The calculations require the optical potentials for the incident and exit channels. These were kept the same as in the FRDWBA calculations described above. The competing channels considered were  $n$ ,  $p$ ,  $\alpha$ , and  $d$  populating the corresponding residual nuclei  $^{22}\text{Na}$ ,  $^{22}\text{Ne}$ ,  $^{19}\text{F}$ , and  $^{21}\text{Ne}$ , respectively, in their discrete and continuum states. The number of discrete levels considered was 18 populated from the emission of neutron, proton, and alpha, respectively, and 12 from the emission of deuteron. The discrete levels were considered up to the maximum energy available for each channel. The missing energy was considered a continuum and the calculations were performed with a level density parameter of  $a = A/7$  ( $A$  is the mass number of the residual nucleus). The spin cutoff parameter was considered as  $\sigma = 3$  for all nuclei as suggested by Gilbert and Cameron [47]. However, the calculation was not very sensitive to the value of  $\sigma$ . The optical potentials for  $n + ^{22}\text{Na}$ ,  $p + ^{22}\text{Ne}$ ,  $\alpha + ^{19}\text{F}$ , and  $d + ^{21}\text{Ne}$  were adopted from Wilmore *et al.* (1964) [48], Perey (1963) [49], and Daehnick (1980) [50], respectively. The HF calculation is shown by the black dotted line in Fig. 3.

It is expected that the FRDWBA model will work best at the most forward angles where there is little compound nucleus reaction contamination. Thus, we fitted the first seven angles where the FRDWBA model best reproduced the



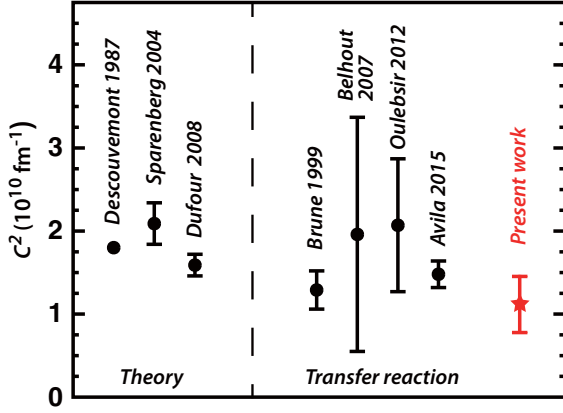


FIG. 4. Comparison of  $\alpha$  particle ANCs of the  $2^+$  (6.92 MeV) subthreshold state of present and previous works. Theoretical values come from Descouvemont (1987) [51], Sparenberg (2004) [52], and Dufour *et al.* (2008) [53]. Experimental data are taken from Brune *et al.* (1999) [25] with  $^{12}\text{C}({}^6\text{Li}, d){}^{16}\text{O}$  and  $^{12}\text{C}({}^7\text{Li}, t){}^{16}\text{O}$  at 2.7–7.0 MeV and 4.75–7.0 MeV, Belhout *et al.* (2007) [28] with  $^{12}\text{C}({}^6\text{Li}, d){}^{16}\text{O}$  at 34 and 50 MeV, Oulebsir *et al.* (2012) [30] with  $^{12}\text{C}({}^7\text{Li}, t){}^{16}\text{O}$  at 28 and 34 MeV and Avila *et al.* (2015) [31] with  ${}^6\text{Li}({}^{12}\text{C}, d){}^{16}\text{O}$  at 5, 7, and 9 MeV.

experimental data. The spectroscopic factor of the  ${}^{16}\text{O}6.9172^+$  state only changed by 2.0% with different range of angles used in the fit and this uncertainty was included in the analysis.

Figure 3 shows the FRDWBA angular distribution of the  $^{12}\text{C}({}^{11}\text{B}, {}^7\text{Li}){}^{16}\text{O}$  reaction together with the experimental data. One sees that the FRDWBA calculation reasonably reproduces the experimental data. The spectroscopic factor ( $S_\alpha$ ) was found to be  $0.139 \pm 0.034$  by the normalization of the FRDWBA calculation to the experimental angular distribution. The ANC ( $C^2$ ) is related to the spectroscopic factor of the state and the single particle ANC ( $b^2$ ) by the relation ( $C^2 = S_\alpha b^2$ ). The ANC of the  $6.9172^+$  state in  ${}^{16}\text{O}$  was extracted to be  $(1.05 \pm 0.26) \times 10^{10} \text{ fm}^{-1}$  using the FRDWBA calculation. The coupled-reaction-channel (CRC) calculation was also performed, which took the coupling between the entrance- and the exit-channels into account. In doing so, the entrance-channel optical potential between  ${}^{11}\text{B}$  and  ${}^{12}\text{C}$  was refitted so that it gave the same elastic scattering cross sections as in the FRDWBA calculations. The resulting spectroscopic factor and ANC were  $0.152 \pm 0.037$  and  $(1.15 \pm 0.28) \times 10^{10} \text{ fm}^{-1}$ . Other coupled channel effects, such as the couplings through inelastic excitations of  ${}^{12}\text{C}$  and  ${}^{16}\text{O}$ , were not taken into account. Such effects have been found to be small in a comprehensive study of the  $^{12}\text{C}({}^6\text{Li}, d){}^{16}\text{O}$  reaction in Ref. [27]. We expect that it is the same in our case.

Finally, the spectroscopic factor and the ANC were determined to be  $0.146 \pm 0.038$  and  $(1.10 \pm 0.29) \times 10^{10} \text{ fm}^{-1}$  by taking the average of the FRDWBA and CRC results. The difference between the results of the FRDWBA and CRC calculations was treated as a part of the total uncertainty. Table I shows the summary of the parameters and the uncertainty budget. We present the comparison of our ANC and previous works in Fig. 4.

#### IV. ASTROPHYSICAL $S_{E2}$ FACTOR OF THE $^{12}\text{C}(\alpha, \gamma)^{16}\text{O}$ REACTION

The astrophysical  $S_{E2}$  factor of the ground-state transitions was derived using the best fits on the basis of the  $R$ -matrix method. The  $R$ -matrix formulas to fit the cross-sections of the scattering data and  $S_{E2}$  under discussion were taken from An *et al.* (2015) [56]. We summarize the formulas here for convenience.

The relevant angular distribution formula for the cross-sections of scattering data is given in Lane *et al.* (1958) [57] by the equation

$$\frac{d\sigma_{\alpha, \alpha'}}{d\Omega_{\alpha'}} = \frac{1}{(2I_1 + 1)(2I_2 + 1)} \sum_{s's'v'v'} |A_{\alpha's'v', \alpha sv'}(\Omega_{\alpha'})|^2, \quad (2)$$

where the  $A_{\alpha's'v', \alpha sv'}$  are the amplitudes of the outgoing waves

$$\begin{aligned} & A_{\alpha's'v', \alpha sv'}(\Omega_{\alpha'}) \\ &= \frac{\sqrt{\pi}}{k_\alpha} \left[ -C_{\alpha'}(\theta_{\alpha'}) \delta_{\alpha's'v', \alpha sv'} + i \sum_{JM l' m'} \sqrt{2l+1} (s l v 0 | J M) \right. \\ & \quad \left. \times (s' l' v' m' | J M) T_{\alpha's' l', \alpha s l}^J Y_{m'}^{(l')}(\Omega_{\alpha'}) \right]. \quad (3) \end{aligned}$$

Several new quantities were introduced in Eq. (3) to define the angular dependence of the cross-section. The term  $-C_{\alpha'}(\theta_{\alpha'})$  represents the Coulomb amplitudes, while the  $Y_{m'}^{(l')}$  are the spherical harmonics functions. Explicitly, the  $T$ -matrix is defined by the  $R$ -matrix components [57], which characterizes the structure information of the  ${}^{16}\text{O}$  compound nucleus.

The  $R$ -matrices are defined as

$$\mathbf{R}_{\alpha's' l', \alpha s l}^J = \sum_{\lambda\mu} \gamma_{\alpha's' l'}^J \gamma_{\alpha s l}^J \mathbf{A}_{\lambda\mu} \delta_{J J_0}, \quad (4)$$

where  $\gamma_{\alpha's' l'}^J$  and  $\gamma_{\alpha s l}^J$  are the reduced-width amplitude of entrance and exit channel, respectively.

The matrix  $\mathbf{A}_{\lambda\mu}$  is defined by its inverse

$$[\mathbf{A}^{-1}]_{\lambda\mu} = (E_\lambda - E) \delta_{\lambda\mu} - \Delta_{\lambda\mu} - \frac{i\Gamma_{\lambda\mu}}{2}, \quad (5)$$

where  $E_\lambda$  is the position of resonance level,  $\Delta_{\lambda\mu}$  is the energy shift,  $\Gamma_{\lambda\mu}$  is the reduced channel width. The energy shift is

$$\Delta_{\lambda\mu} = - \sum_{\alpha s l}^N (S_{\lambda\mu} - B_{\lambda\mu}) \gamma_{\alpha's' l'}^J \gamma_{\alpha s l}^J, \quad (6)$$

where  $S_{\lambda\mu}$  is the shift factor calculated at the channel radius, and  $B_{\lambda\mu}$  is the boundary parameter chosen to equal the shift functions at the energy of the subthreshold state.

For the  $^{12}\text{C}(\alpha, \gamma)^{16}\text{O}$  reaction, the cross-section is determined by the following Eq. (7), which describes ground-state capture in the channel spin representation,

$$\sigma_{\alpha', a} = \frac{\pi}{k_\alpha^2} \sum_{s' l' s' l J} \frac{(2J+1)}{(2I_1+1)(2I_2+1)} |T_{\alpha's' l', \alpha s l}^J|^2, \quad (7)$$

where  $I_1$  and  $I_2$  are the spins of incident particle and target, respectively. The theoretical formulas for error propagation [56]

TABLE II. The resonance parameters used in the  $R$ -matrix fit of the elastic-scattering of  $^{12}\text{C} + \alpha$  [14,54] and astrophysical  $S_{E2}$  factors. The parameters in the brackets are the fixed resonance parameters taken from Tilley *et al.* (1993) [55] except the  $\gamma_\alpha^2$  of 6.917 MeV which adopted the value of the present work.

$J_\pi$	$E_x$ (MeV)	$E_r$ (MeV)	$\gamma_\alpha^2$ or $\Gamma_\alpha$ (keV)	$\Gamma_\gamma$ or $\gamma_\gamma^2$ (keV)
$2_1^+$	6.917	[-0.2449]	$\gamma_\alpha^2 = [18.0 \pm 4.7]^a$	$\Gamma_\gamma = [(9.7 \pm 0.3) \times 10^{-5}]$
$2_2^+$	9.844	[2.684]	$\Gamma_\alpha = 0.71 \pm 19$	$\Gamma_\gamma = (5.7 \pm 0.6) \times 10^{-6}$
$2_3^+$	11.520	4.314	$\Gamma_\alpha = 74 \pm 1$	$\Gamma_\gamma = (6.1 \pm 0.2) \times 10^{-4}$
$2_4^+$	13.020	5.833	$\Gamma_\alpha = 112 \pm 5$	$\Gamma_\gamma = (7.0 \pm 2.0) \times 10^{-4}$
$2_5^+$	15.90	[8.300]	$\gamma_\alpha^2 = [49.3 \pm 2.0]$	$\gamma_\gamma^2 = [(1.8 \pm 0.1) \times 10^{-6}]$
$2_6^+$	16.443	[9.281]	$\gamma_\alpha^2 = [1.1 \pm 0.2]$	$\gamma_\gamma^2 = [(1.9 \pm 0.1) \times 10^{-6}]$
$2_7^+$	Background	22.618	$\gamma_\alpha^2 = 4846 \pm 45$	$\gamma_\gamma^2 = (8.2 \pm 1.0) \times 10^{-3}$

<sup>a</sup>Reduced  $\alpha$ -width from present work.

are adopted to determine the uncertainty of the extrapolated  $S$  factor in our  $R$ -matrix model fitting.

We repeated the fit of the scattering cross-sections of Plaga *et al.* (1987) [54] and Tischhauser *et al.* (2009) [14], with the same  $R$ -matrix parameters of An *et al.* (2015) [56]. Level parameters of the reduced-width amplitude of the entrance channel from the fit were in excellent agreement with those reported in An *et al.* [56].

For the  $R$ -matrix fits of  $S_{E2}$ , we used seven levels associated with the  $^{16}\text{O}$  states at 6.917 ( $2_1^+$ ,  $\lambda = 1$ ), 9.844 ( $2_2^+$ ,  $\lambda = 2$ ), 11.520 ( $2_3^+$ ,  $\lambda = 3$ ), 13.020 ( $2_4^+$ ,  $\lambda = 4$ ), 15.90 ( $2_5^+$ ,  $\lambda = 5$ ), and 16.443 MeV ( $2_6^+$ ,  $\lambda = 6$ ), complemented by a background term ( $2_7^+$ ,  $\lambda = 7$ ). The levels of  $\lambda = 4-7$  were helpful to reduce the uncertainty produced by the distant levels, and also to subsequently improve the fit precision of  $S_{E2}$ . The properties of the relevant states are given in Table II. The properties of these states were fixed in the  $R$ -matrix fits according to Tilley *et al.* (1993) [55], except the reduced  $\alpha$  width  $2_1^+$  (6.917 MeV), which adopted the value of the present work. The observed reduced  $\alpha$  width for the  $2_1^+$  (6.917 MeV) state in the present work was given by

$$\gamma_\alpha^2 = \frac{\hbar^2 R_c}{2\mu} S_\alpha \phi(R_c)^2 = \frac{\hbar^2}{2\mu R_c} C^2 W(R_c)^2, \quad (8)$$

where  $S_\alpha$  and  $C^2$  represent the spectroscopic factor and ANC,  $\phi(R_c)$  and  $W(R_c)$  are the single-particle wave function and the Whittaker function, respectively. The observed reduced  $\alpha$  width,  $\gamma_\alpha^2$ , was converted to the formal channel width in

TABLE III. Details of the fit to each data set of  $S_{E2}$ , including  $\chi^2$  contributions from the literature, normalization parameters, and number of data points (ndp) in each  $\chi^2$  fit.

Reference	Normalization	$\chi^2$	ndp
Plag 2012 [64]	1.03	0.660	4
Makki 2009 [62]	1.03	2.527	4
Ouellet 1996 [59]	0.97	1.305	9
Assunção 2006 [61]	1.00	1.968	20
Kunz 2001 [60]	1.00	1.034	20
Redder 1987 [58]	1.00	3.133	24
Schürmann 2011 [63]	1.03	5.065	7

Eq. (5) during the  $R$ -matrix calculation with the following formula:

$$\Gamma_{\lambda c}^{\text{obs}} = \Gamma_{\lambda c} \left( 1 + \sum_k \gamma_{\lambda k}^2 \frac{dS_k}{dE} \right)_{E_\lambda}^{-1}, \quad (9)$$

which is Eq. (15) in An *et al.* [56]. In the present work,  $\gamma_\alpha^2$  was extracted to be  $18.0 \pm 4.7$  keV at the channel radius of  $R_c = 6.5$  fm. This large radius was chosen to reach the Coulomb asymptotic behavior of  $\phi(R)$  and was also suggested in Oulebsir *et al.* [30] and Brune *et al.* [25]. We also investigated the dependence of the  $S_{E2}(300)$  factor on the channel radius by changing  $R_c$  from 6.0 to 7.0 fm. The uncertainty from  $R_c$  was determined to be 5.4% and was included in the total uncertainty.

The summary of the  $R$ -matrix parameters in the fits is shown in Table II. Table III provides the fitting details such as the normalizations and  $\chi^2$  per data set. In the fitting, the procedure was performed according to the same  $2^+$ -level parameters of this  $R$ -matrix method [56] with the astrophysical  $S$  factors from previous works [58–64]. In general, the data were well fitted where all the levels were accurately described.

The astrophysical  $S_{E2}(300)$  factor of the ground-state transitions was derived to be  $46.2 \pm 7.7$  keV b. The  $R$ -matrix fits are shown in Fig. 5 together with the data from direct

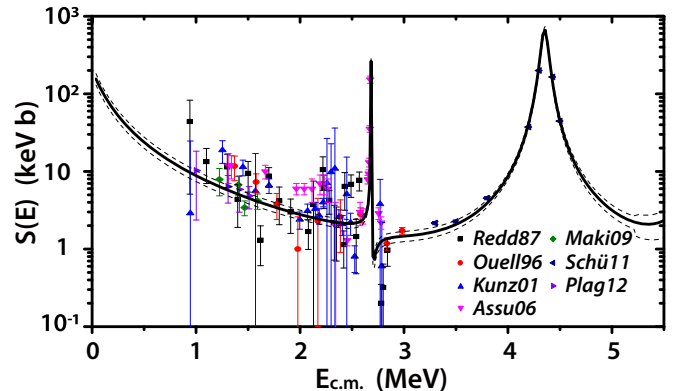


FIG. 5. The comparison of  $R$ -Matrix calculations of  $E2$   $S$  factor with experimental data [58–64]. The solid line is our best  $R$ -matrix fit using our deduced  $\gamma_\alpha^2$  for the 6.917-MeV state, and the dashed lines when using our upper and lower values for  $\gamma_\alpha^2$ .

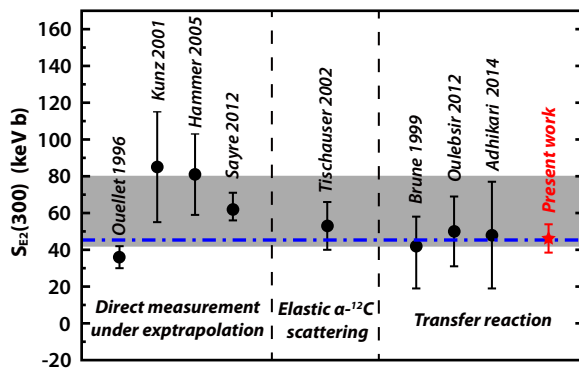


FIG. 6. The  $S_{E2}(300)$  comparison of the present work to previous works [11,16,25,30,59,60,65,66]. The grey shadow represents the compilation value of NACRE II [8]. The blue dot-dashed line is the value in deBoer *et al.* [13].

measurements [58–64]. A comparison of the present  $S_{E2}(300)$  factor to previous results is shown in Fig. 6. One can see that the present result agrees with the compilation of NACRE II ( $61 \pm 19$  keV b) [8] and the most recent compilation by deBoer *et al.* (45.3 keV b) [13].

## V. CONCLUSION

In summary, we measured the angular distribution of the  $^{12}\text{C}(^{11}\text{B}, ^7\text{Li})^{16}\text{O}$  reaction populating the 6.917 MeV  $2^+$

subthreshold state in  $^{16}\text{O}$  using the Q3D magnetic spectrograph at 50 MeV incident energy. The spectroscopic factor and ANC of this state in  $^{16}\text{O}$  were deduced combined a FRD-WBA analysis and a CRC analysis, and then used to calculate the reduced  $\alpha$  width. The uncertainties in the determined  $S_\alpha$ , the reduced  $\alpha$  width and the ANC were also investigated. Finally, we extracted the astrophysical  $S_{E2}(300)$  factor of the ground-state transitions in the  $^{12}\text{C}(\alpha, \gamma)^{16}\text{O}$  reaction to be  $46.2 \pm 7.7$  keV b with the *R*-matrix method. The result for the astrophysical  $S_{E2}(300)$  factor confirms the values obtained in various direct and indirect measurements and is in sound agreement with the compilation of NACRE II ( $61 \pm 19$  keV b) [8] with the center value lower by 17.5 keV b and in good agreement with the most recent compilation by deBoer *et al.* (45.3 keV b) [13], which presents an independent examination of the most important data in nuclear astrophysics.

## ACKNOWLEDGMENTS

The authors thank the staff of the HI-13 tandem accelerator for the smooth operation of the machine. This work was supported by the National Key Research and Development Project under Grant No. 2016YFA0400502, the National Natural Science Foundation of China under Grants No. 11475264, No. 11490561, No. 11375269, and No. 11327508, and the 973 program of China under Grant No. 2013CB834406.

- [1] T. A. Weaver and S. Woosley, *Phys. Rep.* **227**, 65 (1993).
- [2] G. Wallerstein, I. Iben, P. Parker, A. M. Boesgaard, G. M. Hale, A. E. Champagne, C. A. Barnes, F. Käppeler, V. V. Smith, R. D. Hoffman, F. X. Timmes, C. Sneden, R. N. Boyd, B. S. Meyer, and D. L. Lambert, *Rev. Mod. Phys.* **69**, 995 (1997).
- [3] D. Schürmann, L. Gialanella, R. Kunz, and F. Strieder, *Phys. Lett. B* **711**, 35 (2012).
- [4] H. O. U. Fynbo, C. A. Diget, U. C. Bergmann, M. J. G. Borge, J. Cederkäll, P. Dendooven, L. M. Fraile, S. Franchoo, V. N. Fedosseev, B. R. Fulton, W. Huang, J. Huikari, H. B. Jeppesen, A. S. Jokinen, P. Jones, B. Jonson, U. Köster, K. Langanke, M. Meister, T. Nilsson, G. Nyman, Y. Prezado, K. Riisager, S. Rinta-Antila, O. Tengblad, M. Turrion, Y. Wang, L. Weissman, K. Wilhelmsen, J. Äystö, and The ISOLDE Collaboration, *Nature* **433**, 136 (2005).
- [5] L. R. Buchmann and C. A. Barnes, *Nucl. Phys. A* **777**, 254 (2006).
- [6] W. A. Fowler, *Rev. Mod. Phys.* **56**, 149 (1984).
- [7] S. E. Woosley, A. Heger, and T. A. Weaver, *Rev. Mod. Phys.* **74**, 1015 (2002).
- [8] Y. Xu, K. Takahashi, S. Goriely, M. Arnould, M. Ohta, and H. Utsunomiya, *Nucl. Phys. A* **918**, 61 (2013).
- [9] W. Liu, Z. Li, J. He, X. Tang, G. Lian, Z. An, J. Chang, H. Chen, Q. Chen, X. Chen, Z. Chen, B. Cui, X. Du, C. Fu, L. Gan, B. Guo, G. He, A. Heger, S. Hou, H. Huang, N. Huang, B. Jia, L. Jiang, S. Kubono, J. Li, K. Li, T. Li, Y. Li, M. Lugaro, X. Luo, H. Ma, S. Ma, D. Mei, Y. Qian, J. Qin, J. Ren, Y. Shen, J. Su, L. Sun, W. Tan, I. Tanihata, S. Wang, P. Wang, Y. Wang, Q. Wu, S. Xu, S. Yan, L. Yang, Y. Yang, X. Yu, Q. Yue, S. Zeng, H. Zhang, H. Zhang, L. Zhang, N. Zhang, Q. Zhang, T. Zhang, X. Zhang, X. Zhang, Z. Zhang, W. Zhao, Z. Zhao, and C. Zhou, *Sci. China Phys. Mech. Astron.* **59**, 642001 (2016).
- [10] M. Fey, Ph.D. thesis, Universität Stuttgart, Germany, 2004.
- [11] J. W. Hammer, M. Fey, R. Kunz, J. Kiener, V. Tatischeff, F. Haas, J. L. Weil, M. Assunção, C. Beck, C. Boukari-Pelissie, A. Coc, J. J. Correia, S. Courtin, F. Fleurot, E. Galanopoulos, C. Grama, F. Hammache, S. Harissopulos, A. Korichi, E. Krmpotić, D. Le Du, A. Lopez-Martens, D. Malcherek, R. Meunier, P. Papka, T. Paradellis, M. Rousseau, N. Rowley, G. Staudt, and S. Szilner, *Nucl. Phys. A* **752**, 514 (2005).
- [12] J. W. Hammer, M. Fey, R. Kunz, J. Kiener, V. Tatischeff, F. Haas, J. L. Weil, M. Assunção, C. Beck, C. Boukari-Pelissie, A. Coc, J. J. Correia, S. Courtin, F. Fleurot, E. Galanopoulos, C. Grama, F. Hammache, S. Harissopulos, A. Korichi, E. Krmpotić, D. Le Du, A. Lopez-Martens, D. Malcherek, R. Meunier, P. Papka, T. Paradellis, M. Rousseau, N. Rowley, G. Staudt, and S. Szilner, *Nucl. Phys. A* **758**, 363 (2005).
- [13] R. J. deBoer, J. Görres, M. Wiescher, R. E. Azuma, A. Best, C. R. Brune, C. E. Fields, S. Jones, M. Pignatari, D. Sayre, K. Smith, F. X. Timmes, and E. Uberseder, *Rev. Mod. Phys.* **89**, 035007 (2017).
- [14] P. Tischhauser, A. Couture, R. Detwiler, J. Görres, C. Ugalde, E. Stech, M. Wiescher, M. Heil, F. Käppeler, R. E. Azuma, and L. Buchmann, *Phys. Rev. C* **79**, 055803 (2009).

- [15] J. Refsgaard, O. S. Kirsebom, E. A. Djick, H. O. U. Fynbo, M. V. Lund, M. N. Portela, R. Raabe, G. Randisi, F. Renzi, S. Sambri, A. Sytema, L. Willmann, and H. W. Wilschut, *Phys. Lett. B* **752**, 296 (2016).
- [16] S. Adhikari, C. Basu, I. J. Thompson, P. Sugathan, A. Jhinghan, K. S. Golda, A. Babu, D. Singh, S. Ray, and A. K. Mitra, *Phys. Rev. C* **89**, 044618 (2014).
- [17] F. Fleurot, A. M. van den Berg, B. Davids, M. N. Harakeh, V. L. Kravchuk, H. W. Wilschut, J. Guillot, H. Laurent, A. Willis, M. Assunção, J. Kiener, A. Lefebvre, N. de Séréville, and V. Tatischeff, *Phys. Lett. B* **615**, 167 (2005).
- [18] F. Pühlhofer, H. G. Ritter, R. Bock, G. Brommundt, H. Schmidt, and K. Bethge, *Nucl. Phys. A* **147**, 258 (1970).
- [19] D. J. Johnson and M. A. Waggoner, *Phys. Rev. C* **2**, 41 (1970).
- [20] M. E. Cobern, D. J. Pisano, and P. D. Parker, *Phys. Rev. C* **14**, 491 (1976).
- [21] F. D. Becchetti, J. Jänecke, and C. E. Thorn, *Nucl. Phys. A* **305**, 313 (1978).
- [22] F. D. Becchetti, E. R. Flynn, D. L. Hanson, and J. W. Sunier, *Nucl. Phys. A* **305**, 293 (1978).
- [23] A. Cunsolo, A. Foti, G. Pappalardo, G. Raciti, and N. Saunier, *Phys. Rev. C* **18**, 856 (1978).
- [24] F. D. Becchetti, D. Overway, J. Jänecke, and W. W. Jacobs, *Nucl. Phys. A* **344**, 336 (1980).
- [25] C. R. Brune, W. H. Geist, R. W. Kavanagh, and K. D. Veal, *Phys. Rev. Lett.* **83**, 4025 (1999).
- [26] T. L. Drummer, E. E. Bartosz, P. D. Cathers, M. Fauerbach, K. W. Kemper, E. G. Myers, and K. Rusek, *Phys. Rev. C* **59**, 2574 (1999).
- [27] N. Keeley, T. L. Drummer, E. E. Bartosz, C. R. Brune, P. D. Cathers, M. Fauerbach, H. J. Karwowski, K. W. Kemper, B. Kozłowska, E. J. Ludwig, F. Maréchal, A. J. Mendez, E. G. Myers, D. Robson, K. Rusek, and K. D. Veal, *Phys. Rev. C* **67**, 044604 (2003).
- [28] A. Belhout, S. Ouichaoui, H. Beaumevieuille, A. Boughrara, S. Fortier, J. Kiener, J. M. Maison, S. K. Mehdi, L. Rosier, J. P. Thibaud, A. Trabelsi, and J. Vernotte, *Nucl. Phys. A* **793**, 178 (2007).
- [29] S. Adhikari and C. Basu, *Phys. Lett. B* **704**, 308 (2011).
- [30] N. Oulebsir, F. Hammache, P. Roussel, M. G. Pellegriti, L. Audouin, D. Beaumel, A. Bouda, P. Descouvemont, S. Fortier, L. Gaudefroy, J. Kiener, A. Lefebvre-Schuhl, and V. Tatischeff, *Phys. Rev. C* **85**, 035804 (2012).
- [31] M. L. Avila, G. V. Rogachev, E. Koshchiy, L. T. Baby, J. Belarge, K. W. Kemper, A. N. Kuchera, A. M. Mukhamedzhanov, D. Santiago-Gonzalez, and E. Uberseder, *Phys. Rev. Lett.* **114**, 071101 (2015).
- [32] I. J. Thompson, *Comput. Phys. Rep.* **7**, 167 (1988).
- [33] B. Guo, Z. H. Li, M. Lugaro, J. Buntain, D. Y. Pang, Y. J. Li, J. Su, S. Q. Yan, X. X. Bai, Y. S. Chen, Q. W. Fan, S. J. Jin, A. I. Karakas, E. T. Li, Z. C. Li, G. Lian, J. C. Liu, X. Liu, J. R. Shi, N. C. Shu, B. X. Wang, Y. B. Wang, S. Zeng, and W. P. Liu, *Astrophys. J.* **756**, 193 (2012).
- [34] B. Guo, Z. H. Li, Y. J. Li, J. Su, D. Y. Pang, S. Q. Yan, Z. D. Wu, E. T. Li, X. X. Bai, X. C. Du, Q. W. Fan, L. Gan, J. J. He, S. J. Jin, L. Jing, L. Li, Z. C. Li, G. Lian, J. C. Liu, Y. P. Shen, Y. B. Wang, X. Q. Yu, S. Zeng, L. Y. Zhang, W. J. Zhang, and W. P. Liu, *Phys. Rev. C* **89**, 012801 (2014).
- [35] Y. J. Li, Z. H. Li, E. T. Li, X. X. Bai, J. Su, B. Guo, B. X. Wang, S. Q. Yan, S. Zeng, Z. C. Li, J. C. Liu, X. Liu, S. J. Jin, Y. B. Wang, L. Y. Zhang, X. Q. Yu, L. Li, G. Lian, Q. W. Fan, and W. P. Liu, *Eur. Phys. J. A* **48**, 13 (2012).
- [36] Z. H. Li, Y. J. Li, J. Su, B. Guo, E. T. Li, K. J. Dong, X. X. Bai, Z. C. Li, J. C. Liu, S. Q. Yan, Y. B. Wang, S. Zeng, G. Lian, B. X. Wang, S. J. Jin, X. Liu, W. J. Zhang, W. Z. Huang, Q. W. Fan, L. Gan, Z. D. Wu, and W. P. Liu, *Phys. Rev. C* **87**, 017601 (2013).
- [37] B. Guo, X. C. Du, Z. H. Li, Y. J. Li, D. Y. Pang, J. Su, S. Q. Yan, Q. W. Fan, L. Gan, Z. Y. Han, E. T. Li, X. Y. Li, G. Lian, J. C. Liu, C. J. Pei, L. H. Qiao, Y. P. Shen, Y. Su, Y. B. Wang, S. Zeng, Y. Zhou, and W. P. Liu, *EPJ Web Conf.* **109**, 04003 (2016).
- [38] D. Y. Pang, Y. L. Ye, and F. R. Xu, *Phys. Rev. C* **83**, 064619 (2011).
- [39] Y. P. Xu and D. Y. Pang, *Phys. Rev. C* **87**, 044605 (2013).
- [40] B. A. Brown, *Phys. Rev. C* **58**, 220 (1998).
- [41] G. R. Satchler, *Nucl. Phys. A* **329**, 233 (1979).
- [42] E. Bauge, J. P. Delaroche, and M. Girod, *Phys. Rev. C* **63**, 024607 (2001).
- [43] E. Liatard, J. F. Bruandet, F. Glasser, S. Kox, T. U. Chan, G. J. Costa, C. Heitz, Y. E. Masri, F. Hanappe, R. Bimbot, D. Guillemaud-Mueller, and A. C. Mueller, *Europhys. Lett.* **13**, 401 (1990).
- [44] Y. Funaki, H. Horiuchi, and A. Tohsaki, *Prog. Part. Nucl. Phys.* **82**, 78 (2015).
- [45] Y. P. Shen *et al.* (unpublished).
- [46] E. Sheldon and V. Rogers, *Comput. Phys. Commun.* **6**, 99 (1973).
- [47] A. Gilbert and A. Cameron, *Can. J. Phys.* **43**, 1446 (1965).
- [48] D. Wilmore and P. E. Hodgson, *Nucl. Phys.* **55**, 673 (1964).
- [49] F. Perey, *Phys. Rev.* **131**, 745 (1963).
- [50] W. W. Daehnick, J. D. Childs, and Z. Vrcelj, *Phys. Rev. C* **21**, 2253 (1980).
- [51] P. Descouvemont, *Nucl. Phys. A* **470**, 309 (1987).
- [52] J.-M. Sparenberg, *Phys. Rev. C* **69**, 034601 (2004).
- [53] M. Dufour and P. Descouvemont, *Phys. Rev. C* **78**, 015808 (2008).
- [54] R. Plaga, H. Becker, A. Redder, C. Rolfs, H. Trautvetter, and K. Langanke, *Nucl. Phys. A* **465**, 291 (1987).
- [55] D. R. Tilley, H. R. Weller, and C. M. Cheves, *Nucl. Phys. A* **564**, 1 (1993).
- [56] Z.-D. An, Z.-P. Chen, Y.-G. Ma, J.-K. Yu, Y.-Y. Sun, G.-T. Fan, Y.-J. Li, H.-H. Xu, B.-S. Huang, and K. Wang, *Phys. Rev. C* **92**, 045802 (2015).
- [57] A. Lane and R. Thomas, *Rev. Mod. Phys.* **30**, 257 (1958).
- [58] A. Redder, H. Becker, C. Rolfs, H. Trautvetter, T. Donoghue, T. Rinckel, J. Hammer, and K. Langanke, *Nucl. Phys. A* **462**, 385 (1987).
- [59] J. M. L. Ouellet, M. N. Butler, H. C. Evans, H. W. Lee, J. R. Leslie, J. D. MacArthur, W. McLatchie, H.-B. Mak, P. Skensved, J. L. Whitton, X. Zhao, and T. K. Alexander, *Phys. Rev. C* **54**, 1982 (1996).
- [60] R. Kunz, M. Jaeger, A. Mayer, J. W. Hammer, G. Staudt, S. Harissopulos, and T. Paradellis, *Phys. Rev. Lett.* **86**, 3244 (2001).
- [61] M. Assunção, M. Fey, A. Lefebvre-Schuhl, J. Kiener, V. Tatischeff, J. W. Hammer, C. Beck, C. Boukari-Pelissie, A. Coc, J. J. Correia, S. Courtin, F. Fleurot, E. Galanopoulos, C. Grama, F. Haas, F. Hammache, F. Hannachi, S. Harissopulos, A. Korichi, R. Kunz, D. LeDu, A. Lopez-Martens, D. Malcherek, R. Meunier, T. Paradellis, M. Rousseau, N. Rowley, G. Staudt,



- S. Szilner, J. P. Thibaud, and J. L. Weil, [Phys. Rev. C \*\*73\*\*, 055801 \(2006\)](#).
- [62] H. Makii, Y. Nagai, T. Shima, M. Segawa, K. Mishima, H. Ueda, M. Igashira, and T. Ohsaki, [Phys. Rev. C \*\*80\*\*, 065802 \(2009\)](#).
- [63] D. Schürmann, A. D. Leva, L. Gialanella, R. Kunz, F. Strieder, N. D. Cesare, M. D. Cesare, A. D'Onofrio, K. Fortak, G. Imbriani, D. Rogalla, M. Romano, and F. Terrasi, [Phys. Lett. B \*\*703\*\*, 557 \(2011\)](#).
- [64] R. Plag, R. Reifarth, M. Heil, F. Käppeler, G. Rupp, F. Voss, and K. Wisshak, [Phys. Rev. C \*\*86\*\*, 015805 \(2012\)](#).
- [65] P. Tischhauser, R. E. Azuma, L. Buchmann, R. Detwiler, U. Giesen, J. Görres, M. Heil, J. Hinnefeld, F. Käppeler, J. J. Kolata, H. Schatz, A. Shotter, E. Stech, S. Vouzoukas, and M. Wiescher, [Phys. Rev. Lett. \*\*88\*\*, 072501 \(2002\)](#).
- [66] D. B. Sayre, C. R. Brune, D. E. Carter, D. K. Jacobs, T. N. Massey, and J. E. O'Donnell, [Phys. Rev. Lett. \*\*109\*\*, 142501 \(2012\)](#).